Z. Phys. D – Atoms, Molecules and Clusters 19, 47–50 (1991)

Atoms, Molecules
Zeitschrift für Physik D and Clusters

The influence of shells, electron thermodynamics, and evaporation on the abundance spectra of large sodium metal clusters

S. Bjørnholm, J. Borggreen, O. Echt*, K. Hansen, J. Pedersen, and H.D. Rasmussen

The Niels Bohr Institute, University of Copenhagen, DK-4000 Roskilde, Denmark

Received 10 September 1990

Abstract. Measurements of the mass abundance spectra of sodium clusters containing up to 600 atoms are presented. The clusters are produced in a seeded supersonic expansion of Ar or Kr gas, and the spectra are obtained by a time-of-flight technique. The sawtooth features in the spectra are interpreted as evidence of a regular spherical shell structure with magic numbers, N_0, scaling approximately with the cube root of the number of sodium atoms. Altogether twelve shell closings are observed, $N_0 = 2$, 8, 20, 40, 58, 92, 138, 196, 260, 344, 440 and 558. There is also a pronounced odd-even staggering all the way up to $N = 70$. The experimentally observed intensity changes for the clusters around the magic numbers are discussed in terms of the electronic free energy, $F(N)$, calculated at finite temperature, and the second differences of the free energy $\Delta_2 F(N) = F(N-1) - 2F(N) + F(N+1)$. The processes behind the non-uniform abundance distributions, and the thermodynamics of finite electron systems with non-uniform level spacings are discussed on this basis.

PACS: 36.40; 35.20.Wg; 03.65.-w

Introduction

This contribution addresses questions related to the existence of periodically varying properties of clusters of simple metals, initially discovered by W.D. Knight et al. [1] (with Na- and K-clusters) and by I. Katakuse et al. [2] (with Cu, Ag, and Au-clusters).

We have measured abundance spectra of sodium clusters, generated by seeded adiabatic expansion, up to cluster sizes N corresponding to 600 atoms. The results obtained, are in qualitative agreement with the shell structure predicted theoretically by Nishioka et al. [3, 4] and by Brack et al. [5, 6] as presented at this conference.

A more quantitative comparison of the first difference of the logarithm of the experimental intensities $\Delta_1 \ln I_N = \ln(I_{N+1}/I_N)$ with the calculated [5] second difference of Helmholtz' free energy, $F = E - TS$, including electronic contributions, shows striking similarities. Based on these similarities, a picture of the processes behind the production of the experimentally observed, non-uniform abundance distributions is conjectured. It involves the following assumptions:

(i) Insufficient removal of the heat of condensation during expansion leads to a broad and initially structureless distribution of large clusters at near-boiling temperatures.
(ii) During flight for about one millisecond, the cluster distribution forms an evaporative ensemble [7, 8], cooling to 400–500 K by monomer evaporation, as shown by Bréchignac et al. [9].
(iii) Within size intervals corresponding to at least one major shell, the cooling will occur in secular equilibrium all the time; i.e. the turnover, or the product of decay constant and abundance, will be the same irrespective of size.
(iv) The decay constant can be cast in the form $k_N = \nu A \exp(\Delta_1 F(N-1)/kT)$ with $\nu \simeq 10^{13}\,\mathrm{s}^{-1}$, A the number of atoms in the surface, and $\Delta_1 F(N-1)$ the first difference of the Helmholtz free energy [10].
(v) The transition state for monomer evaporation can be identified with the final, fully dissociated state; i.e. the effective activation energy $-\Delta_1 F(N-1)$ for evaporation can be obtained from calculations of the free energy of the clusters in their equilibrium state [5, 6].
(vi) The 'true' shell gaps in the electron eigenvalue spectra are smaller than calculated theoretically for spherical droplets. A single phenomenological scaling parameter can account for this in a crude way.

The magnitude of the shell-structure modulations of the abundance spectra are measurable although they become quite weak for large clusters. The above assumptions are helpful, if not necessary, as steps towards a more complete understanding of the experimental mass spectra.

* *Present address*: Physics Department, University of New Hampshire, Durham, NH 03834, USA

In addition to shell modulations, the abundance spectra also exhibit pronounced odd-even alternations in the size intervals between major shells. This aspect is discussed in B.R. Mottelson's contribution to this conference [11].

Experimental procedure and results

The experiments were performed with beams of free flying clusters produced by adiabatic expansion from a hot oven into vacuum. In the oven, argon or krypton gas at stagnation pressures of $(4-8)\cdot 10^5$ Pa is seeded with saturated sodium vapor at 700–800°C, i.e. partial sodium pressures of $(1-4)\cdot 10^4$ Pa. The diameter of the cylindrical expansion nozzle is 0.07 mm and its length about 0.15 mm. With the aid of skimmers and a differential pumping stage, the sodium cluster beam is introduced into a 3 m long flight line. Ionization of the clusters is achieved with ultraviolet light from a 1 kW xenon lamp. The photon energy is centered at 3.9 eV, with a band width (FWHM) of 1.0 eV. This ensures an ionization probability that varies smoothly with size, and at the same time negligible heating of the ionized species [12, 13]. After ionization the clusters are analysed by time-of-flight mass spectrometry to obtain the abundance variations as a function of size, N. The time-of-flight spectrometer consists of a 5–10 kV acceleration stage, deflection plates that sweep the ionized d.c. beam across a narrow slit at about 3 kHz picking out narrow bunches with a well defined starting time for the flight time measurements, a reflectron to compensate for small velocity variations, and a channeltron ion detector. The arrival times are recorded with a multi-hit time-to-digital converter and passed to a computer that records the mass spectrum. The mass resolution is typically $M/\Delta M = 1200$. After background subtraction each mass peak is integrated to give the total mass abundance I_N.

The top panels in Fig. 1 show the measured abundance distributions, I_N. On the left hand side are results obtained with argon carrier gas, to the right results with krypton gas. In both cases, the spectra have a bell-shaped envelope modulated by a saw-tooth like fine structure. The envelopes reflect the global kinetics of cluster growth during the high-pressure phases of the expansion, while the saw-tooth structures are believed to emerge as a result of subsequent evaporation–and cooling–in flight from isolated clusters [7–9].

The local features of the abundance spectra can be displayed more clearly by taking the logarithmic difference of the I_N-values:

$$\Delta_1 \ln I_N = \ln(I_{N+1}/I_N) \approx 2(I_{N+1} - I_N)/(I_{N+1} + I_N) \quad (1)$$

The lower left panel in Fig. 1 is a plot of this quantity. It eliminates the influence of the global shape. On the other hand, the smearing of the saw-teeth occurring at higher shells tends to reduce the value of the logarithmic difference strongly. This is compounded by the general decrease in relative magnitude of the saw-tooth steps with increasing N. As a result, statistical uncertainties begin to obscure the shell effects. On the lower right hand panel we have plotted a generalized logarithmic difference,

$$(\Delta_1 \ln I_N)_{K_0} = \frac{\sum_{K=0}^{K_0} \frac{2(I_{N+1+K} - I_{N-K})(2K+1)}{(I_{N+1+K} + I_{N-K})}}{\sum_{K=0}^{K_0} (2K+1)^2} \quad (2)$$

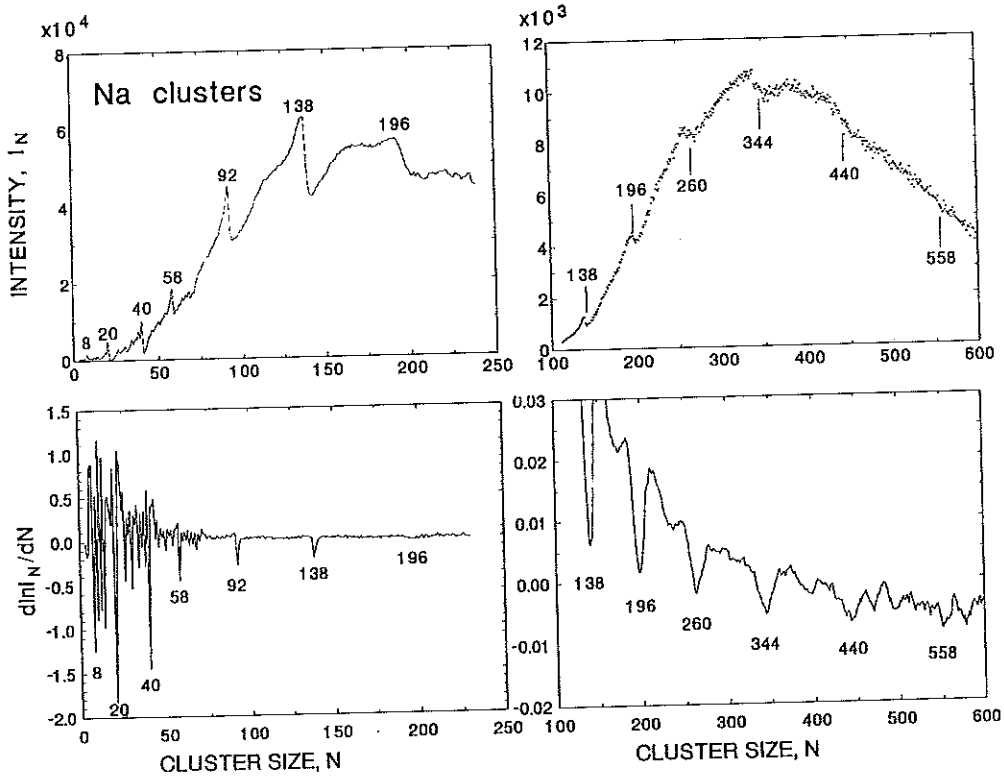

Fig. 1. Top panels: Abundance distributions for sodium clusters produced by adiabatic expansion and measured by time-of-flight mass spectrometry: left: carrier gas Ar; right: carrier gas Kr. Bottom panels: Logarithmic differences of results in top panels. Bottom left: Eq. (1), bottom right: Eq. (2) with $K_0 = 8$. (The last magic number, 558, requires a higher K_0-value to stand out unambiguously)

with $K_0 = 8$. Averaging over mass intervals $2K_0 + 1$, comparable to the smearing, makes the shell dips stand out clearly again.

Discussion

The magic numbers determined experimentally are indicated in Fig. 1 and discussed in [14] in relation to the theoretical study of shells in large quantum systems [3, 4]. Similarly the odd-even staggering, visible in the top left panel of Fig. 1, is discussed in [11].

The two top panels in Fig. 2 present the experimental data once more in the form of the first logarithmic difference $\Delta_1 \ln I_N$, given by (1) or (2), this time multiplied by $kT = 0.043$ eV, corresponding to an estimated [9] final temperature of about 500 K. In addition, the data for the heavier mass interval (right panel) has been linearized by subtracting a smooth curve drawn through the mid-shell segments of the data Fig. 1 (lower right panel).

These experimental quantities are compared to the results of theoretical calculations of the negative of the second difference of the free energy $-\Delta_2 F(N)$, displayed in the two lower panels.

$$\Delta_2 F(N) = F(N-1) - 2F(N) + F(N+1). \tag{3}$$

The second differences are obtained from free energies, calculated for electrons in an external spherical potential of the Woods-Saxon type [3, 4], with $kT = 0.043$ eV. The method used is described in [5, 6]. However, prior to the calculation of $F(N)$, the eigen-energies have been arbitrarily scaled down by a factor 2.5. This reduction accounts in a crude, phenomenological way for the reduction in magnitude of the empirical shell gaps [15, 16], compared to the calculated ones.

The energy scales in Fig. 2 are the same for the experimental and the theoretical results. Furthermore it should be noted that the units on the right hand panels (large clusters) are one hundred times smaller than on the left hand panels (small clusters). In other words, the amplitude of the logarithmic difference $\Delta_1 \ln I_N$ (top panels) varies by more than a factor of hundred in going from shell no. 3 ($N_0 = 20$) to shell no. 9 ($N_0 = 260$). At the same time, the dips at the magic numbers become more and more broad. As can be seen, the calculation (lower panels) simulates the experiment over this very large dynamic range quite well, and also the qualitative changes in the shell dips. The calculation is therefore likely to contain the essential elements of a more complete theory, designed to describe the experimental abundance distributions in detail. The key elements are those listed *(i)–(vi)* in the introduction.

Most important is the conjecture of hotly formed clusters *(i)*, decaying as an evaporative ensemble of isolated clusters *(ii)*, as opposed to (local) chemical equilibrium established by collisions. The assumption of secular equilibrium *(iii)* and the specific form of the decay constant *(iv)* provides the link between $kT\Delta_1 \ln I_N$ and $\Delta_2 F(N)$. A constant turnover *(iii)* implies that for all N

$$I_N k_N = \text{const.} \tag{4}$$

hence, with $k_N = \nu A \exp(\Delta_1 F(N-1)/kT)$

$$\ln I_N = -\ln k_N = -\Delta_1 F(N-1)/kT \tag{5}$$

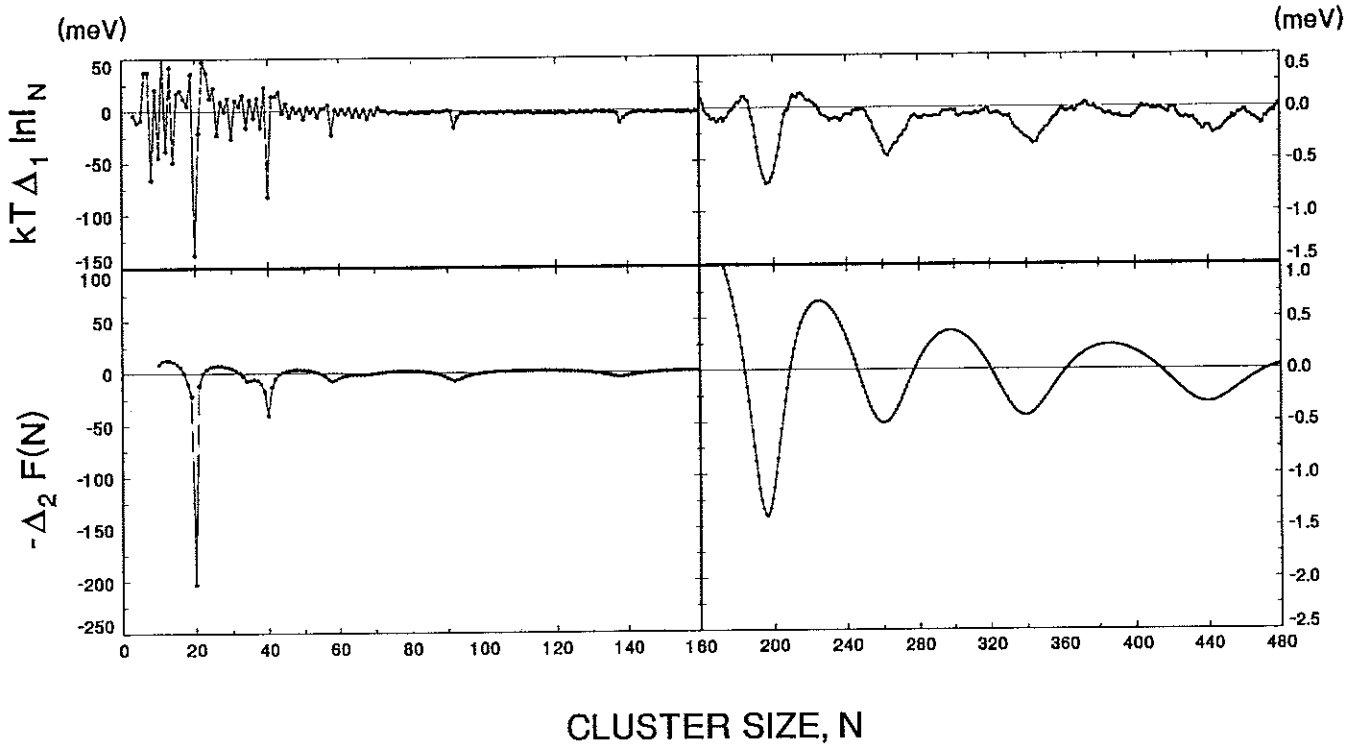

Fig. 2. Top panels: First logarithmic derivative of measured abundances, Fig. 1, multiplied by kT, corresponding to 500 K. Bottom panels: Theoretically calculated second differences of the (electronic) free energy, Eq. (3); Refs. [5, 6]

apart from additive constants or smoothly varying quantities. These are eliminated by forming differences

$$kT\Delta_1 \ln I_N = -\Delta_1 F(N) + \\ + \Delta_1 F(N-1) \equiv -\Delta_2 F(N) \quad (6)$$

To be meaningful, a comparison of the measured $kT\Delta_1 \ln I_N$ values with the free energy differences $-\Delta_2 F(N)$, calculated for the individual spherical equilibrium states, requires that the free energy of transition state is identical with that of the final state *(v)*. Finally, a compression of the single particle energy scale *(vi)* by a factor of about 2.5 is required to match observations and calculations as shown in Fig. 2. This phenomenological factor mocks up all the perturbations, in the form of deformations [17], thermal shape oscillations, pseudopotentials, effective mass effects etc., that conspire to make the shell gaps in the eigenvalue spectrum less pronounced than in the idealized model calculation [3–6].

Conclusion

A closer study of the experimental abundance modulations of sodium cluster distributions across a large size interval reveals that the observable shell effects are strongly influenced by temperature. The valence electrons, in equilibrium with the ions, absorb finite amounts of heat. The amount of heat absorbed and the entropy varies strongly and also periodically with size [5, 6]. The net effect is a strong attenuation of the observable shell effects for large clusters, compared to zero-temperature predictions. It is nevertheless possible to measure the shell effects by mass abundance spectrometry.

Special thanks are due to W.D. Knight for guiding the authors into the field of experimental cluster research during a sabattical stay at the Niels Bohr Institute in 1988. Theoretical discussions with M. Brack, T. Døssing, B. R. Mottelson and H. Nishioka are gratefully acknowledged. We also thank D. Radford for developing our peak fitting program. This work has been supported by The Carlsberg Foundation, The Danish Research Academy, The Danish National Science Research Council, Julie Damm's Fund, Novo's Fund, the SARC-Fund and Thomas B. Thriges Fund.

References

1. Knight, W.D., Clemenger, K., de Heer, W.A., Saunders, W.A., Chou, M.Y., Cohen, M.L.: Phys. Rev. Lett. **52,** 2141 (1984); de Heer, W.A., Knight, W.D., Chou, M.Y., Cohen, M.L.: Solid State Phys. **40,** 93 (1987)
2. Katakuse, I., Ichihara, T., Fujita, Y., Matsuo, T., Sakurai, T., Matsuda, H.: Int. J. Mass Spectrom. Ion Processes **67,** 229 (1985)
3. Nishioka, H., Hansen, K., Mottelson, B. R.: Phys. Rev. B. (to appear)
4. Nishioka, H.: Z. Phys. D – Atoms, Molecules and Clusters (1991) (this issue)
5. Brack, M., Genzken, O., Hansen, K.: Phys. Rev. B. (submitted for publication)
6. Brack, M., Genzken, O., Hansen, K.: Z. Phys. D – Atoms, Molecules and Clusters (1991) (this issue)
7. Klots, C.E.: J. Chem. Phys. **92,** 5864 (1988)
8. Klots, C.E.: Z. Phys. D – Atoms, Molecules and Clusters (1991) (this issue)
9. Brechignac, C., Cahuzac, Ph., Leygnier, J., Weiner, J.: J. Chem. Phys. **90,** 1492 (1989)
10. Døssing, T.: Private communication (to be published)
11. Mottelson, B.R.: Z. Phys. D – Atoms, Molecules and Clusters (1991) (this issue)
12. de Heer, W.A.: Ph.D. Thesis, University of California, Berkely (1985)
13. The authors are grateful to W.A. de Heer and W.D. Knight for detailed advice on the construction of the cluster machine
14. Bjørnholm, S., Borggreen, J., Echt, O., Hansen, K., Pedersen, J., Rasmussen, H. D.: Phys. Rev. Lett. **65,** 1627 (1990)
15. Bergmann, T., Martin, T. P.: J. Chem. Phys. **90,** 2848 (1989)
16. Homer, M.L., Persson, J.L., Honea, E.C., Whetten, R.L.: Preprint (1990)
17. Ekardt, W., Penzar, Z.: Phys. Rev. B. **38,** 4273 (1988)